8 Foreland basin evolution and the growth of an orogenic wedge

8.1 Introduction

Peripheral foreland basin systems (DeCelles and Giles, 1996) result from the flexural downbending of continental lithosphere in response to tectonic and topographic loading during continent-continent collision (Price, 1973). The spatial evolution of the associated depozones, i. e., wedge-top, foredeep, forebulge and backbulge (Fig. 8.1) and their respective sedimentary infill, is strongly dependent on (i) the effective elastic thickness (Te) of the involved lithospheres; (ii) the level of horizontal stresses; (iii) the magnitude of the loads imposed on the foreland by the orogenic wedge and the subducted lithospheric slab; (iv) the dip-angle of the latter; (v) the rate and direction of convergence; (vi) the amount of erosion of the orogenic wedge and the dispersal system within the foreland and (vii) eustasy (Beaumont, 1981; Turcotte and Schubert, 2002; Allen et al., 1991; Sinclair, 1997b; Ziegler et al., 2002). Numerous field studies have demonstrated that almost all foredeeps evolve from an underfilled to a filled or overfilled depositional state (Covey, 1986; Sinclair, 1997a). The underfilled state is characterised by deep-marine (Flysch type) sediments, high thrust advance rates, and low exhumation rates. In contrast, the overfilled state shows shallow marine to continental (Molasse type) deposits and a dominance of exhumation versus frontal advance of the orogen (Sinclair and Allen, 1992). Classically, the Flysch to Molasse transition is interpreted as recording the migration of the thrust wedge and the associated foredeep over the hinge-

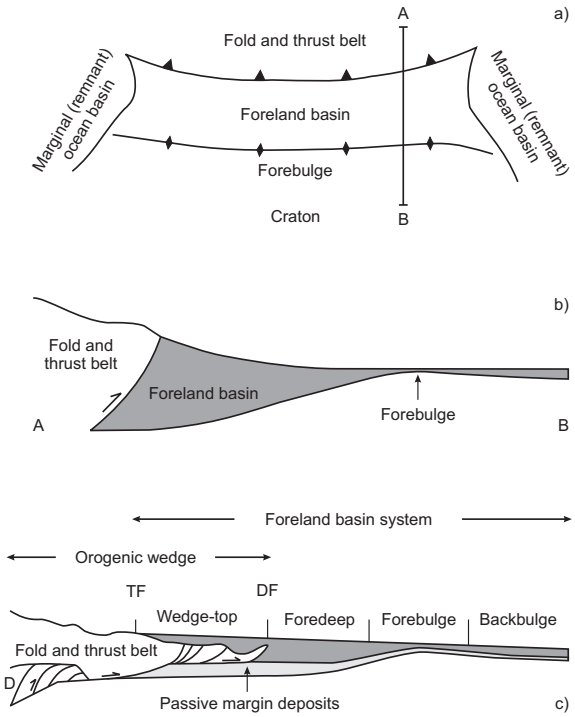

Figure 8.1: (a) Schematic map view of a foreland basin, bounded longitudinally by a pair of marginal ocean basins. The scale is not specified, but would be of the order of 10^2 to $10^3\,km$. Vertical line at right indicates the orientation of a cross-section that would resemble what is shown in (b). (b) The generally accepted notion of foreland-basin geometry in transverse cross-section. Note the unrealistic geometry of the boundary between the basin and the thrust belt. Vertical exaggeration is of the order of 10 times. (c) Schematic cross-section depicting a revised concept of a foreland basin system, with the wedge-top, foredeep, forebulge and backbulge depozones shown at approximately true scale. Topographic front of the thrust belt is labeled TF. The foreland basin system is shown in dark grey; area in light grey indicates passive margin deposits, which are incorporated into (but not shown within) the fold-thrust belt toward the left of diagram. A schematic duplex (D) is depicted in the hinterland part of the orogenic wedge. Note the substantial overlap between the front of the orogenic wedge and the foreland basin system. Modified after DeCelles and Giles (1996).

line of the inherited passive margin of the underthrusted plate (Dewey, 1982). Numerical simulations in conjunction with field studies in the Swiss Alps however, suggest that the rate of frontal advance of the orogenic wedge and the sediment transport coefficient (K) are the main control on

the state of the foredeep infill, whereas an increase of the flexural rigidity or the surface slope of the orogenic wedge is only of minor importance (Sinclair et al., 1991; Sinclair, 1997b).

Additionally, most forward modelling studies, which are aimed at unravelling the influence of the above parameters on the stratigraphic architecture of foreland basins (Flemings and Jordan, 1990; Jordan and Flemings, 1991; Sinclair et al., 1991; Crampton and Allen, 1995; Galewsky, 1998; Allen et al., 2001; Clevis et al., 2004), assume that the respective orogenic load results from either a lithospheric scaled fault-bend fold (Flemings and Jordan, 1990) or from a pro-wedge sensu Willett et al. (1993). However, sandbox simulations of bivergent orogens (like this study) have demonstrated that strain is partitioned between the pro- and the retro-wedge. It follows that processes acting either upon or within the retro-wedge control the load distribution within the pro-wedge as well, which in turn influences the geometry of the pro-foredeep. Consequently, cause and effect would be considerably offset in space.

Thus, the purpose of this study, which is based on scaled-sandbox simulations as well as analytical considerations, is twofold. First, we explore how the lateral growth of an orogenic wedge controls the spatio-temporal evolution of the pro-foredeep and thus the Flysch to Molasse transition. Second, we focus on the influence of the coupling between the pro- and the retro-wedge on the evolution of the pro-foredeep. In order to address both issues we consider a reference experiment (9.05) and one experiment with pro- and another with retro-wedge erosion (9.09, 9.06). Finally, sedimentary basins and thus foreland basins provide the most significant sources of energy-related commodities, such as hydrocarbons, coal, uranium and many metals (Kyser and Hiatt, 2003). Consequently, the formulation of conceptual models and the detection of far-field relations may help to constrain future exploration strategies.

8.2 Method

Time series of the horizontal distance between the deformation front of the pro-wedge and the singularity $[L_{fp}/H_0]$ as well as the height of the axial-zone above the singularity $[H/H_0]$ provide an approximation of the triangular shape of the pro-wedge throughout its evolution. Although these data represent dimensionless lengths, they are scaled by 10^5, a factor commonly used in sandbox experiments (e. g., Malavieille, 1984; Storti et al., 2000). Both converted time series (L and H) are used to calculate the flexure of a hypothetic foreland lithosphere in response to orogenic loading for each time (convergence) step according to Turcotte and Schubert (2002):

$$V_0 = W\rho_{orogen}gLH \tag{8.1}$$

$$\alpha = \left(\frac{4D}{(\rho_m - \rho_s)g}\right)^{1/4} \tag{8.2}$$

$$w_0 = \frac{\left(\frac{4D}{(\rho_m-\rho_s)g}\right)^{3/4} V_0}{4D} \tag{8.3}$$

$$w_x = w_0 e^{-x/\alpha} cosx/\alpha \tag{8.4}$$

whereby V_0 is the vertical load in N, W is the width of the hypothetical orogen = $1m$, L is the converted length of the pro-wedge in m, H is the converted height of the axial-zone above the singularity in m, α is the flexural parameter, D is the flexural rigidity of the plate, chosen to be $10^{22}\,Nm$, g is the acceleration due to gravity ($9.81\,m/s^2$), ρ_{orogen} is the density of a hypothetical orogen ($2600\,kg/m^3$), ρ_m is the density of the mantle ($3300\,kg/m^3$), ρ_s is the density of sediments, filling the foredeep ($2300\,kg/m^3$), w_0 is the deflection of the plate at $x = 0$ and $w(x)$ is the deflection of the plate at point x. Density values are

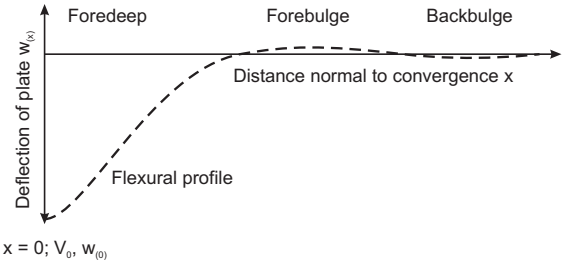

Figure 8.2: Theoretical deflection of an elastic broken plate under a line load applied at its end. Modified from Allen and Allen (2005).

mean values and have been taken from Turcotte and Schubert (2002). A schematic flexural profile is shown in figure (8.2). As in previous modelling studies (Karner and Watts, 1983; Sinclair et al., 1991; Crampton and Allen, 1995; Roddaz et al., 2005) orogenic overthrusting of the foreland plate is simulated by two-dimensional a priori loading of a broken elastic plate. Flexural response to loading is treated as instantaneous, since the response time for isostatic adjustment is on the order of 10^3 to 10^5 years (Crampton and Allen, 1995).

Lateral migration of the pro-wedge gravity-center was not taken into account. This would have resulted in slight changes of the foredeep geometry only. Effects of horizontal stresses on the foreland basin system are neglected, since they would only slightly magnify the effects of flexure and would not change the overall geometries. Sea level variations would have a similar negligible effect on plate flexure (Crampton and Allen, 1995). The influence of different flexural rigidities on the foreland basin system is well known (e. g., Flemings and Jordan, 1989; Sinclair et al., 1991). High flexural rigidities lead to the formation of a broad, shallow depression with a low, wide forebulge, whereas low flexural rigidities give rise to a deep, narrow peripheral trough and a relatively high forbulge. This means that, as the load advances across the plate, the onset of subsidence at a given point on the profile will be later, and the rate of subsidence higher for a low compared to a high flexural rigidity (Sinclair et al., 1991; Crampton and Allen, 1995). In a sediment-filled basin the forebulge will be less high, because the flexural response to the sediment load interferes with the one from the orogenic load, resulting in a less well developed forebulge. Since we are interested in the Flysch to Molasse transition, we assume that the foredeep is completely filled with sediments.

8.3 Results and discussion

Flexural profiles derived from the above calculations image three out of the four depozones associated with foreland basin systems, i. e., the foredeep, the forebulge and the backbulge. Although, the shape of the flexural profile depends on a multitude of factors as outlined above, the corresponding magnitudes of either downbending or uplift agree with field observations. According to DeCelles and Giles (1996) foredeep depozones are commonly 2 to $8\,km$ thick, forebulges are $\sim 10\,m$ to several $100\,m$ high and backbulges are generally not deeper than $200\,m$. Maximum calculated values are $2\,km$, $150\,m$ and $20\,m$, respectively (Fig. 8.3). The temporal evolution of the flexural profiles further indicates that:

i. During early stages of orogenic evolution, incremental deepening of the foredeep as well as incremental uplift of the forebulge is high, but decreases with further convergence. This is to be expected, since both the width and the height of the pro-wedge, are best described by a power law (section 5.3.7).

ii. Each thrust initiation phase is followed by a deepening of the foredeep and uplift of the forebulge, an observation, which has been documented by Jordan and Flemings (1991) as well. Thrust episodes lead to depth changes of $\sim 1\,m$ of the backbulge region.

iii. For a given lateral position, thrust induced change of the depth of the foredeep decreases with increasing proximity to the orogen. In

contrast, each thrust event has a profound effect on the height of the forebulge, which is consistent with previous analytical studies (e. g., Jordan and Flemings (1991)).

Although associated with lower magnitudes, these three phenomena can be as well observed in both the pro- and the retro-wedge erosion case (Fig. 8.3b, c). Furthermore, we found that also retro-wedge erosion has a significant influence on the spatio-temporal evolution of the pro-foredeep. The above results confirm thus, the expected and well established link between the evolution of orogenic belts and their foreland basin system (DeCelles and Giles, 1996). There are however, some implications, which deserve further discussion.

The CCW concept predicts and sandbox simulations confirmed that the lateral and vertical growth of an orogenic wedge follows a power law (Dahlen, 1990; Mulugeta and Koyi, 1992; Hoth et al., 2006). The disagreement between theoretically predicted and experimentally derived power law coefficients is not considered here, but was discussed in section (5.3.7). If the width and the height of an orogenic belt grow proportional to the convergence (t) by $t^{0.5}$, then the respective incremental change, which is described by the first derivation ($-0.5t^{0.5}$), decreases with time. It follows that the associated increase of the load of the orogenic wedge onto its foreland and thus the resulting increase of the deflection decreases through time as well. At the same time however, the surface of the wedge, prone to be eroded, grows proportional to the convergence (t) by $2t^{0.5}$ and is thus twice as fast as the lateral and vertical growth. If one further assumes a constant erosion rate of the wedge and a constant sedimentation rate within the foredeep, a change from underfilled (fast addition of new accommodation), to overfilled (slow addition of new accommodation) would result. This transition would be thus an emergent consequence of the imposed kinematic boundary conditions. We therefore propose a two-staged evolutionary model. During early stages of convergence the rate of orogenic growth/advance is high and so is the rate of flexure induced subsidence within the foredeep. Debris derived from the orogen is deposited in a deep and probably underfilled foredeep (Flysch-type). At a later stage of convergence the rate of flexure induced subsidence within the foredeep decreases. The latter is successively filled and may reach a point in its evolution where all sediments are bypassed (overfilled or Molasse-type). There is thus no need to invoke a halt of convergence or a slab breakoff to explain the Flysch to Molasse transition. A slowdown of thrust front advance associated with the Flysch to Molasse transition has been documented for the Swiss Alps and the Longmen Shan Thrust Belt (Sinclair, 1997b; Yong et al., 2003; Kempf and Pfiffner, 2004) and has been postulated for the Pyrenees as well (Labaume et al., 1985).

The influence of erosion on the orogen-foredeep system would be twofold. First, erosion controls the geometry and the propagation of an orogenic wedge and thus determines the incremental addition of load responsible for the flexure. Second, erosion provides the debris with which the foredeep is filled. Consequently, intense erosion of the pro-wedge promotes the Flysch to Molasse transition within the pro-foredeep and would thus lead to a short-lived underfilled foreland basin system. This might explain the scarcity of early Flysch deposits in the foredeep of the Himalayas, Taiwan and the Pyrenees, which were subject to intense erosion on their respective pro-wedges (Covey, 1986; Fitzgerald et al., 1999; Najman et al., 2004).

We further highlight the far-field connection between retro-wedge erosion and the spatio-temporal evolution of the pro-foredeep. In a previous section (6.2) we demonstrated that retro-wedge erosion influences thrust activity within the pro-wedge and thus seismicity. Consequently, retro-wedge erosion does also change the load distribution of the pro-wedge and thus the flexure of the pro-lithosphere. Given that the magnitude of strain transfer between the pro- and the retro-

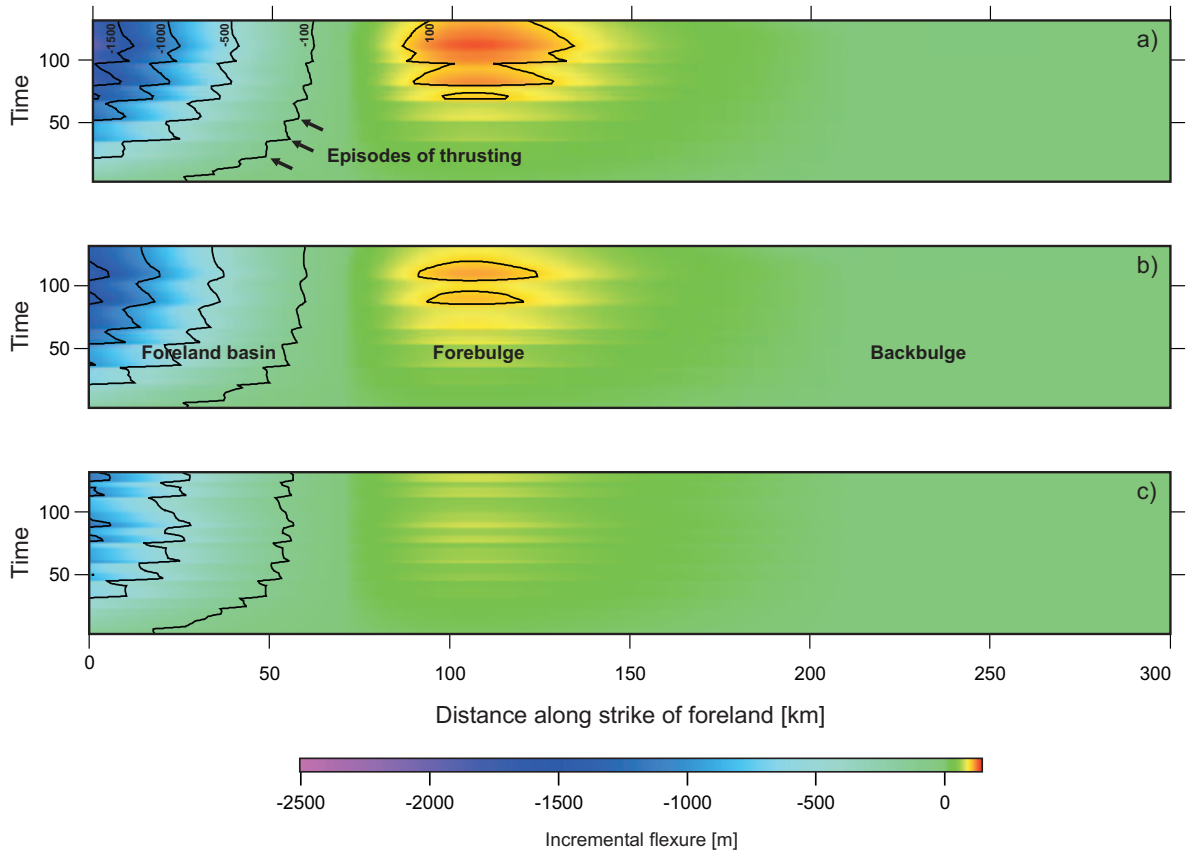

Figure 8.3: Spatio-temporal evolution of hypothetic foreland basins. See text for derivation. (a) Reference experiment; Distributed erosion of: (b) Retro-wedge, (c) Pro-wedge.

wedge decreases while the former grows laterally, the above far-field influence might be only detectable during early stages of convergence.

Episodes of thrust activity result in transgression-regression cycles, where transgressions on the distal side correlate with regressions on the proximal or forebulge side (Fig. 8.3, Flemings and Jordan (1990)). Such a scenario is supported by observations from the Karoo Basin, which formed in response to the advance of the Cape Fold Belt (Catuneanu and Elango, 2001). The Late Permian to Early Triassic Balfour Formation, which was deposited during the overfilled phase of the Karoo Basin, consists of six third-order depositional sequences separated by prominent subaerial unconformities. In the absence of any evidence for a climatic or eustatic forcing, these six sequences are thought to result from thrust episodes within the Cape Fold Belt (Catuneanu and Elango, 2001). The average duration of each cycle was calculated to be $0.66 Ma$.

Similarly, thrusting within the Swiss Alps might explain the stepwise nature of transgressions within the North Alpine Foreland basin between $50 Ma$ and $37 Ma$ (Kempf and Pfiffner, 2004). This observation has been previously attributed to crustal-scaled inhomogeneities, which tend to focus plate bending (Waschbusch and Royden, 1992). Thus, further analysis of the kinematic evolution of the advancing Alpine orogen is required to address this issue.

Migration of an orogen towards its foreland is associated with a coevally migrating flexural wave. In submarine foreland basins forebulges are preferred sites for carbonate platforms to develop (Crampton and Allen, 1995; DeCelles and Giles, 1996). Consequently, sites of active carbonate deposition may first experience uplift and erosion, associated with karstification and are finally drowned due to the submergence beneath the photic zone (Galewsky, 1998). Carbonate platform drowning is controlled by the maximum upward growth potential of the platform-building organisms and the rate of sea level rise relative to the platform. The latter depends on the tectonically induced subsidence and on eustatic sea-level variations. It follows that the interplay between deformation and surface processes within the advancing orogen controls the duration of forebulge uplift and thus the degree of karstification (Crampton and Allen, 1995) and finally the rate of drowning. In the North Alpine Foreland basin, karstification below the drowning unconformity surface reaches up to $100\,m$ down into the limestones, resulting in an extensive interconnected system of macropores, which may finally form hydrocarbon reservoirs (Crampton and Allen, 1995). Thus, the understanding of the eroding orogen may finally help to predict forbulge plays. Furthermore, forebulge unconformities are preferred sites of Mississippi Valley Type deposits (Leach et al., 2001; Bradley and Leach, 2003). Their formation might be induced by an eroding orogen, hundreds of kilometers away.